JOURNAL OF CATALYSIS 157, 76–86 (1995)

Activation of Nitric Oxide by Heteropoly Compounds: Structure of Nitric Oxide Linkages in Tungstophosphoric Acid with Keggin Units

N. Chen and R. T. Yang[1]

Department of Chemical Engineering, State University of New York at Buffalo, Buffalo, New York 14260

Received January 12, 1995; revised June 2, 1995; accepted July 26, 1995

The heteropoly compound $H_3PW_{12}O_{40} \cdot 6H_2O$ is composed of anions of the Keggin structure, $(PW_{12}O_{40})^{-3}$, linked by $H_5O_2^+$ to form a body-centered cubic (bcc) structure. The water linkages can be substituted readily by NO linkages at 50–230°C at low NO concentrations (i.e., under flue gas conditions) to form $H_3PW_{12}O_{40} \cdot 3NO$. A substantial fraction of the absorbed NO is decomposed into N_2 upon rapid heating of the NO-linked compound. The bond energy for the NO linkages is on the order of 25 kcal/mol, based on the TPD results. From the XRD data, the bcc structure is preserved in the NO-saturated compound, except the bcc lattice constant is decreased by 4.2% upon substitution. The IR spectrum of $H_3PW_{12}O_{40} \cdot 3NO$ shows a single band for NO at 2270 cm^{-1}. Based on the IR results, the TPD data, and the literature information on the nitrosonium ion (NO^+), the linkage in the NO saturated compound is an ionic form of protonated NO, $(NOH)^+$. Bond length calculations yield a value of 11.74 Å for the ionic linkage, which is in close agreement with the bcc lattice constant of 11.68 Å obtained from XRD. The structure closely resembles that of $Cs_3PW_{12}O_{40}$. The NO molecule is activated upon absorption in the heteropoly compound by protonation, resulting in weakening of the N–O bond. The activation of NO, combined with rapid heating (so desorption can occur at high temperatures), results in N_2 production. The result that the sodium salt $Na_3PW_{12}O_{40}$ cannot absorb NH_3 or NO suggests that the ability to interact with H^+ is a prerequisite to form linkages in heteropoly compounds. © 1995 Academic Press, Inc.

INTRODUCTION

Heteropoly acids and salts are a class of compounds that have attracted much scientific interest. Because of their unique structures and the resulting acidic and redox properties, they have been studied as possible catalysts for a variety of reactions. It has been found recently in our laboratory that the tungstophosphoric heteropoly acid can effectively absorb NO at the flue gas temperatures, and upon rapid heating (to 400–450°C), the absorbed NO is effectively decomposed into N_2 (1). For example, at 150°C and a space velocity of 5,000 h^{-1}, 70% of the NO in a simulated flue gas was absorbed by the fixed bed of the heteropoly compound particles. After NO saturation, upon heating the bed to 450°C at a heating rate of 150°C/min, 68.3% of the absorbed NO was decomposed into N_2. The heating step was also accomplished in the simulated flue gas. Hence nearly 50% of the NO in the simulated flue gas was decomposed into N_2 by this two-step procedure. This potentially most significant application of the heteropoly compounds led us to investigate the nature of the bonding between NO and $H_3PW_{12}O_{40}$. In the present study, *in situ* FTIR, XRD, and TPD were employed to determine the structure of the NO-bonded $H_3PW_{12}O_{40}$. An understanding of the structure of the bonded NO can also lead to more effective means to decompose NO.

$H_3PW_{12}O_{40}$ belongs to a large class of heteropoly compounds, the structures of which are well understood (2). The crystal structure of the $PW_{12}O_{40}$ anion belongs to the Keggin structure (3) of $XM_{12}O_{40}$. In this structure, 12 MO_6 octahedra surround a central XO_4 tetrahedron, where M is usually W or Mo and X can be P, As, Si, Ge, B, and others. Although the structures of the heteropoly anions (e.g., the Keggin structure) are well defined and stable (termed primary structure), the structures by which the Keggin units are linked together (termed secondary structure) are less understood. Water is usually the linkage molecule, and a distinct X-ray diffraction pattern is seen for $H_3PW_{12}O_{40} \cdot 6H_2O$, where the Keggin units are linked by $H^+(H_2O)_2$ bridges resulting in the X-ray diffraction pattern. The water molecules can be easily replaced by a number of polar molecules such as alcohols and amines (4). The proximity of protons and heteropoly anions gives rise to interesting catalytic activities, particularly for the acid-catalyzed redox reactions (4–22). During the catalyzed reactions, the secondary structure usually undergoes changes where the reactant molecules substitute the water linkages and are activated, thus the reactions take place in the bulk (rather than on the surface) of the heteropoly compounds. Consequently, an understanding of the struc-

[1] Present address for all correspondence: Department of Chemical Engineering, University of Michigan, Ann Arbor, MI 48109.

0021-9517/95 $12.00

ture and bonding of the linkages in the secondary structure is necessary for the understanding of the reaction mechanism.

Our work (1) has been followed by a study on the absorption of NO_x in heteropoly compounds, also at 150°C (23), which was published after the submission of this paper.

EXPERIMENTAL

The heteropoly compound used in this study was reagent grade powder of $H_3PW_{12}O_{40} \cdot xH_2O$ supplied by Alfa Products, Ward Hill, MA. $Na_3PW_{12}O_{40} \cdot xH_2O$ was prepared from $H_3PW_{12}O_{40} \cdot xH_2O$ by ion exchange with a solution of Na_2CO_3, following the procedure reported in the literature (16, 24). NO and NH_3 were supplied in the premixed forms of 0.86% (vol.) NO in N_2 and 0.97% NH_3 in N_2, by Matheson Gas Products. They were further diluted to 3000 ppm in all experiments. All other gases were from the Linde Division as described elsewhere (1). The BET N_2 (77 K) surface area of $H_3PW_{12}O_{40} \cdot 6H_2O$ (formed after heating and N_2 purge) was measured with a Quantasorb analyzer, and was approximately 10 m^2/g.

The IR spectra were measured with a Nicolet Model Impact 400 FTIR Spectrometer, with 1 cm^{-1} resolution. *In situ* spectra were obtained by employing an IR cell which was connected to a gas mixing and flow system. The sample could be heated *in situ* to up to 500°C. The IR sample holder was a Si or CaF_2 plate. The heteropoly compound was first dissolved in water and the compound was dispersed on the plate by drying the solution on the plate at 80°C. In all *in situ* treatments in the IR cell, the following concentrations were used (at atmospheric pressure): 3000 ppm NO, 3000 ppm NH_3, 2% H_2O and 2% O_2, with either N_2 or He as the inert carrier.

X-ray powder diffraction patterns were measured with a Siemens powder diffractometer with Cu $K\alpha$ source. The transmission mode was employed except where high resolution was needed. For lattice constant calculations, high resolution patterns were obtained by using the reflection mode, and pure Si powder was used as the internal standard for calibration. Although no *in situ* capabilities were available, measures were taken to minimize air exposure, as similar procedures are reported in the literature (16). The samples treated with different gases were sealed in glass vials under the same gas atmospheres, and a Mylar film and mineral oil were employed to protect the sample from contacting the ambient air during the XRD measurements.

The reactor described earlier (1) was used to measure the TPD profiles. The reactor was a quartz tube with temperature-programmed control, and was connected to a gas handling system. The NO/NO_x concentrations in the effluent gas were monitored and recorded by a chemiluminescent NO/NO_x analyzer (Thermoelectron Model 10). Helium was used in TPD. A quadrupole mass spectrometer (UTI Model 100 C) was used to measure the N_2 concentration in the effluent gas in selected runs.

RESULTS

NO Linkage Formation and Stoichiometry

It has been shown in our earlier work that the water linkages in the secondary structure were replaced by NO linkages when $H_3PW_{12}O_{40} \cdot 6H_2O$ was exposed to 1,000 ppm NO in He in a wide temperature range, e.g., 100–230°C (1). Although it was observed that O_2 strongly accelerated the substitution reaction, and the presence of H_2O was also helpful, it is not clear whether the substitution could take place in the absence of O_2 and H_2O. The mechanism of NO substitution is under further study.

Based on the amount of NO absorbed (in a bed of the heteropoly compound), the net weight change during substitution (from TGA data), and the literature information on other substitutions, it was concluded that the reaction followed the stoichiometry (1)

$$H_3PW_{12}O_{40} \cdot 6H_2O \xrightarrow{NO} H_3PW_{12}O_{40} \cdot 3NO. \quad [1]$$

TPD of NO

The NO-saturated heteropoly compound, $H_3PW_{12}O_{40} \cdot 3NO$, was subjected to TPD experiments. The TPD profiles at three heating rates are shown in Fig. 1.

Upon heating the $H_3PW_{12}O_{40} \cdot 3NO$ compound, a fraction of the NO linkages evolved as N_2, and a strong dependence of the amount of N_2 on the heating rate was established in our earlier work (1). By heating at different heating rates from 150 to 450°C, the fractions of NO linkages that evolved as N_2 were 68.3% at 150°C/min, 59.6% at 100°C/min, and 35.4% at 50°C/min (1). In the TPD experiments, relatively slow heating rates were used for the purpose of determining the bond strengths of the NO linkages. The highest heating rate used in the TPD experiments was 10°C/min. Mass spectrometry analysis (for N_2 concentration history) in conjunction with the chemiluminescent analysis (for NO concentration history) were performed for the TPD effluent at 10°C/min heating rate. The results showed that only 11% of NO linkages evolved as N_2. Therefore, the activation energy for desorption calculated from the TPD results was a good indication of the bond energy for the NO linkages.

As shown in Fig. 1, for all three heating rates, only a single peak in NO evolution appeared. There was also a very small peak near 300°C, likely due to adsorbed NO. The TPD profiles were asymmetric, indicating that the desorption of NO linkages was first order (25). The maximum desorption temperature (T_m) increased with heating rate (β). The activation energy for breaking the NO linkages (E) can be calculated from (25)

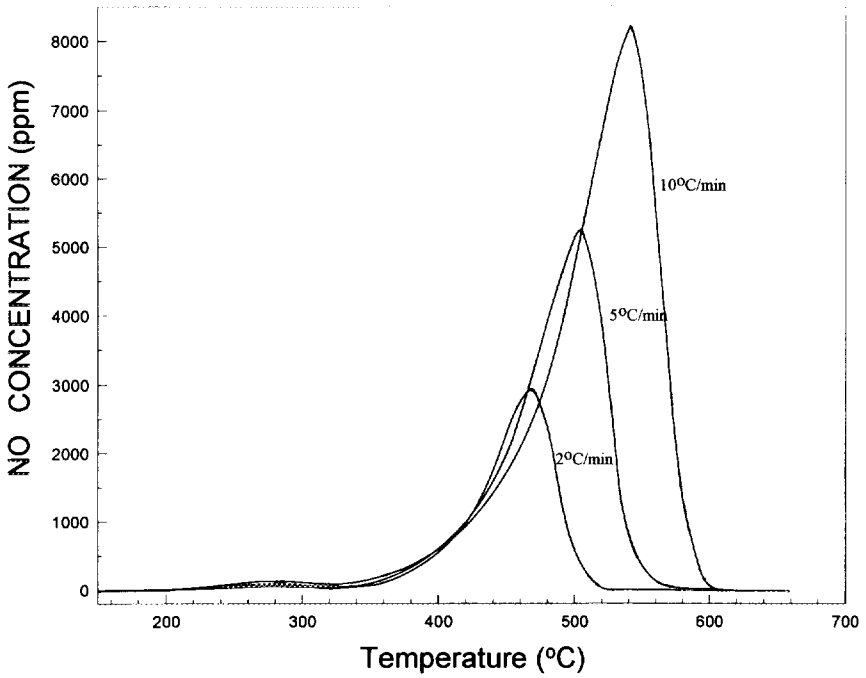

FIG. 1. TPD profiles of $H_3PW_{12}O_{40} \cdot 3NO$ at three heating rates. (See Table 1 for details.)

$$\frac{d\,ln\,(T_m^2/\beta)}{d(1/T_m)} = \frac{E}{R}. \qquad [2]$$

The peak temperatures were 467°C (at 2°C/min), 501°C (at 5°C/min), and 534°C (at 10°C/min). A plot based on Eq. [2] yielded $E = 25.5$ kcal/mol. For chemisorption with no readsorption, this value of activation energy for desorption is equal to the heat of desorption or the bond energy (25). In our case, the bond energy for the NO linkages to the Keggin anions was equal to or less than 25.5 kcal/mol.

The chemiluminescent NO/NO_x analyzer can detect either NO or NO_x, where $NO_x = NO + NO_2$. A separate TPD run was made, at 5°C/min heating rate, to measure the amount of NO_2 evolved upon heating. The NO_x profile showed identical features as the NO profile (see Fig. 1) except that the concentration of NO_x was higher than NO by approximately 3%. The result showed that the decomposition product was essentially NO, with only 3% NO_2.

Stoichiometry by Nitrogen Mass Balance: 3NO vs $2NO_2$ Linkages

Based on the TGA (i.e., weight change) results upon substitution of H_2O linkages by NO_x linkages in the secondary structure, we concluded the stoichiometry shown by reaction (1). However, the TGA results could also be interpreted (23) by the following reaction:

$$H_3PW_{12}O_{40} \cdot 6H_2O \xrightarrow[O_2]{NO} H_3PW_{12}O_{40} \cdot 2NO_2. \qquad [3]$$

To resolve this important question, a detailed nitrogen mass balance based on TPD and gas product analyses was made.

First, two corrections were needed. Based on the TGA results (1), the total dehydration of $H_3PW_{12}O_{40} \cdot xH_2O$ yielded a 10% weight loss. Thus, 10% needed to be subtracted from the weight of the starting sample. As mentioned, N_2 was also formed in the TPD experiments, and the amount of N_2 increased with heating rate. At 10°C/min heating rate, 11% of the NO linkages evolved as N_2. Mass spectrometry measurements (for N_2) were not performed for the heating rates of 5°C/min and 2°C/min. Reasonable estimates for the fractions of NO that evolved as N_2 were 5% and O% for 5°C/min and 2°C/min, respectively.

The results on the nitrogen mass balance are shown in Table 1. From these results, it is clear that the stoichiometry $H_3PW_{12}O_{40} \cdot 3NO$ is the correct one, and $H_3PW_{12}O_{40} \cdot 2NO_2$ is incorrect.

XRD Patterns and Lattice Constant for $H_3PW_{12}O_{40} \cdot 3NO$

The XRD powder patterns for $H_3PW_{12}O_{40} \cdot 6H_2O$ and $H_3PW_{12}O_{40} \cdot 3NO$ are compared in Fig. 2. Both patterns were obtained with samples purged in N_2 at room temperature. The Na^+-exchanged salt did not produce a well-defined XRD at the room temperature. It was noted by Hayashi and Moffat (24) that calcination at 150°C was needed for the Na^+ salt to produce a clear XRD pattern. However, their salt contained some residual proton (~0.3 H^+ per

TABLE 1

Nitrogen Mass Balance from TPD Runs for Stoichiometry of NO_x Linkages

	Run 1	Run 2	Run 3
$H_3PW_{12}O_{40} \cdot xH_2O$ weight (g)	1.0	1.0	1.0
$H_3PW_{12}O_{40}$ weight (g)	0.9	0.9	0.9
Heating rate (°C/min)	2.0	5.0	10.0
NO evolved[a] (NO/Keggin unit)	3.1	2.8	2.4
N_2 evolved (N_2/Keggin unit)	0.0	0.07[b]	0.13[c]
Total NO as linkages (NO/Keggin unit)	3.1	2.9	2.7

Note. The carrier gas was He, at 250 ml/min.

[a] As discussed in text, NO_2 and NO_x are negligible.

[b] Estimated from Run 3 and the data discussed in text.

[c] Measured by mass spectrometry.

TABLE 2

Body-Centered Cubic Lattice Constants (a) for Secondary Structure Calculated from XRD Patterns

	$H_3PW_{12}O_{40} \cdot 6H_2O$			$H_3PW_{12}O_{40} \cdot 3NO$		
(hkl) face:	(110)	(222)	(332)	(110)	(222)	(332)
2θ	10.1	25.4	34.6	10.7	26.4	36.2
d spacing (Å)	8.76	3.51	2.59	8.27	3.38	2.48
a (Å)	12.37	12.16	12.15	11.70	11.71	11.63
Avg. a (Å)		12.23			11.68	

Keggin unit). It is not clear whether a fully Na^+-exchanged salt would produce an XRD pattern.

The XRD patterns shown in Fig. 2 were essentially the same except that all peaks were shifted toward higher 2θ values for $H_3PW_{12}O_{40} \cdot 3NO$. This result indicated that the NO-linked heteropoly compound retained the body-centered cubic (bcc) secondary structure of the water-linked form. However, the lattice constant of the secondary structure was decreased. The bcc lattice constants were calculated from the three strongest reflections, and the results are listed in Table 2. The bcc lattice constant of the $H_3PW_{12}O_{40} \cdot 6H_2O$ averaged around 12.2 Å, which was in agreement with the value 12.15 Å reported by Brown *et al.* (26). The average bcc lattice constant calculated from three reflections for $H_3PW_{12}O_{40} \cdot 3NO$ was 11.68 Å, which represented approximately 4% shrinkage of the secondary structure upon substitution of $6H_2O$ per Keggin anion by 3NO per Keggin anion.

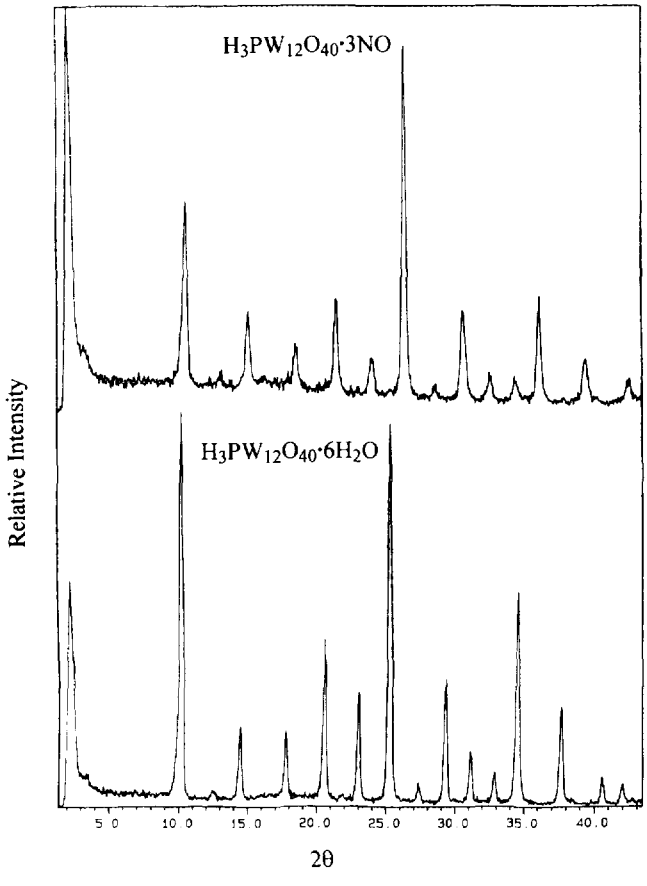

FIG. 2. XRD powder patterns for $H_3PW_{12}O_{40} \cdot 6H_2O$ and $H_3PW_{12}O_{40} \cdot 3NO$.

IR Spectra

While the XRD pattern reveals the crystalline structure (or spatial arrangement) of the secondary structure of the heteropoly compound, the IR spectrum provides vibrational frequency information on the $XM_{12}O_{40}$ anion as well as that of the linkages between the anions.

The following concentrations (at 1 atm total pressure) were used in the IR cell: 3,000 ppm NO, 3,000 ppm NH_3, 2% H_2O, and 2% O_2, with N_2 or He as the inert carrier. The heat treatments were done in the inert carrier.

The IR spectra of $H_3PW_{12}O_{40} \cdot 6H_2O$ treated at various temperatures up to 150°C are shown in Fig. 3. The spectrum at 25°C was that of $H_3PW_{12}O_{40} \cdot 6H_2O$ and the band assignments have been reported in the literature (27, 28). The band at 980 cm^{-1} was due to the stretching vibration of $W = O_t$ where O_t denotes the terminal oxygen in the Keggin structure, and the band at 1080 cm^{-1} was assigned to the asymmetric stretching vibration of the central PO_4 tetrahedron. The bands at 1620 cm^{-1} and 1710 cm^{-1} were attributed to the bending vibrations of, respectively, H_2O and H_3O^+ in the linkages in the secondary structure (29). The band for H_3O^+ was clearly the dominant one. The broad band at 3200 cm^{-1} was due to the OH stretching vibration in the H_2O linkages. Upon heating to 150°C, some H_2O linkages still remained, while the band at 980 cm^{-1} split into 970 and 1000 cm^{-1}. The splitting of the

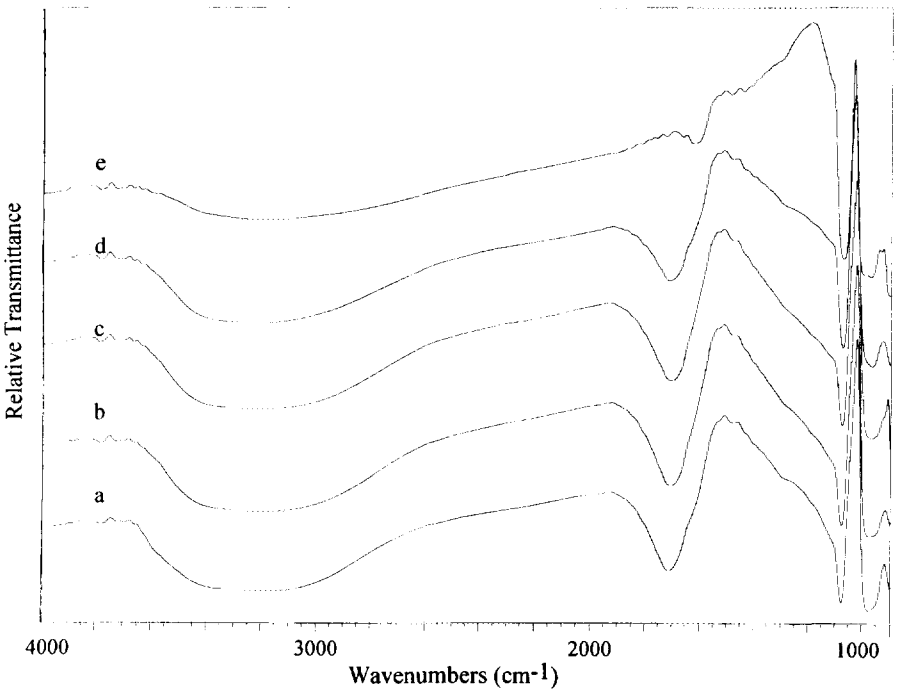

FIG. 3. IR spectra of $H_3PW_{12}O_{40} \cdot 6H_2O$ treated in N_2 at the following temperatures: (a) 25°C; (b) 80°C; (c) 100°C; (d) 120°C; and (e) 150°C.

W = O_t band was interpreted as the result of a shift of the H^+ proton from the terminal oxygen to the corner and edge shared oxygen atoms on the Keggin structure, causing a change in the environment for the terminal oxygen (30).

Figure 4 shows the IR spectra of $Na_3PW_{12}O_{40} \cdot xH_2O$ upon successive heat treatments to 150°C. The bands for H_2O in the sodium salt were quite different from that of the acid. Only the 1620 cm^{-1} band was present for the bending mode, and the stretching vibrations were at higher frequencies than that of the acid, and were typical of that of the hydrate. The absence of the 1710 cm^{-1} band indicated the lack of H_3O^+ in the sodium salt. Moreover, the H_2O bands became very weak at 120°C. No changes were observed for the bands between 900 and 1100 cm^{-1}, indicating the same structure for the Keggin anion.

Ammonia absorption and desorption experiments were performed on both $H_3PW_{12}O_{40} \cdot 6H_2O$ and the sodium salt. The IR spectra are shown in Figs. 5 and 6. The results with $H_3PW_{12}O_{40} \cdot 6H_2O$ (Fig. 5) were in general agreement with that reported in the literature (31). The strong IR band at 1450 cm^{-1} was characteristic of the bending mode of NH_4^+ (32), with the corresponding stretching frequencies at near 3200 cm^{-1}. NH_3 was bonded much more strongly than H_2O with the protons, as shown by the higher temperature (of 450°C) that was needed for desorption of NH_3. Figure 6 shows the IR spectra of the $Na_3PW_{12}O_{40}$ salt upon NH_3 treatment and subsequent heat treatments. The appearance of the 1450 cm^{-1} band upon NH_3 treatment at 25°C indicated that there was some Brønsted acidity; however, this Brønsted acidity was not strong enough to form H_3O^+ upon H_2O treatment (Fig. 5).

Moreover, the Brønsted acidity in the sodium salt was weak enough so that NH_4^+ could desorb readily at 200°C (Fig. 6). More interestingly, upon cooling the sodium salt to 25°C after NH_4^+ desorption at 200°C, it was no longer possible to pick up NH_3 in the salt at 25°C (Fig. 6). The weak Brønsted acidity was lost upon ammonia desorption at 200°C. A detailed study on heat treatment indicated that a substantial amount of the Brønsted acidity was actually lost at 150°C.

The IR spectra for NO absorbed in $H_3PW_{12}O_{40} \cdot 6H_2O$ are shown in Fig. 7. These spectra were taken *in situ*, without using the KBr pellet. In our earlier work, we reported an IR spectrum using the KBr pellet of the NO-saturated heteropoly compound and showed three IR absorption bands for NO, 1295 cm^{-1}, 1390 cm^{-1}, and 2270 cm^{-1} (1). In the *in situ* spectra shown in Fig. 7 (without KBr), only one band due to NO was seen, that at 2270 cm^{-1}. Also included in Fig. 7 is a spectrum of a KBr pellet exposed to NO at 150°C. It is then clear that the two bands at 1295 and 1390 cm^{-1} that we reported earlier were due to the interaction between the NO that was absorbed in the heteropoly compound and the KBr. The 2270 cm^{-1} band could be assigned only to a nitrosonium ion (NO^+), as will be discussed. Figure 7 also shows that the absorbed NO in the heteropoly acid was bonded quite strongly, and it was not desorbed until the temperature was raised to nearly 400°C.

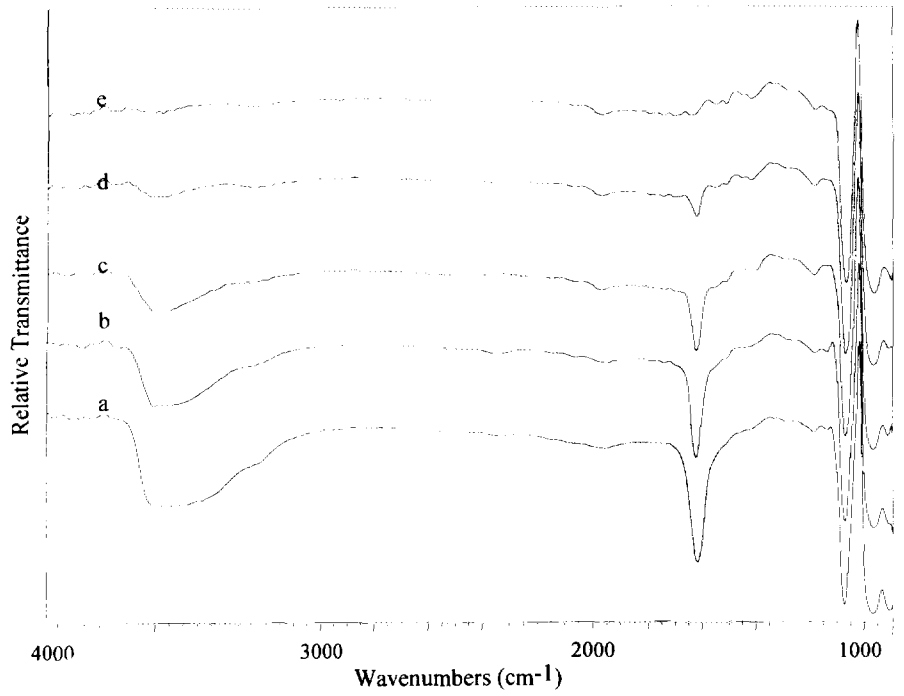

FIG. 4. IR spectra of $Na_3PW_{12}O_{40} \cdot nH_2O$ treated in N_2 at the following temperatures: (a) 25°C; (b) 80°C; (c) 100°C; (d) 120°C; and (e) 150°C.

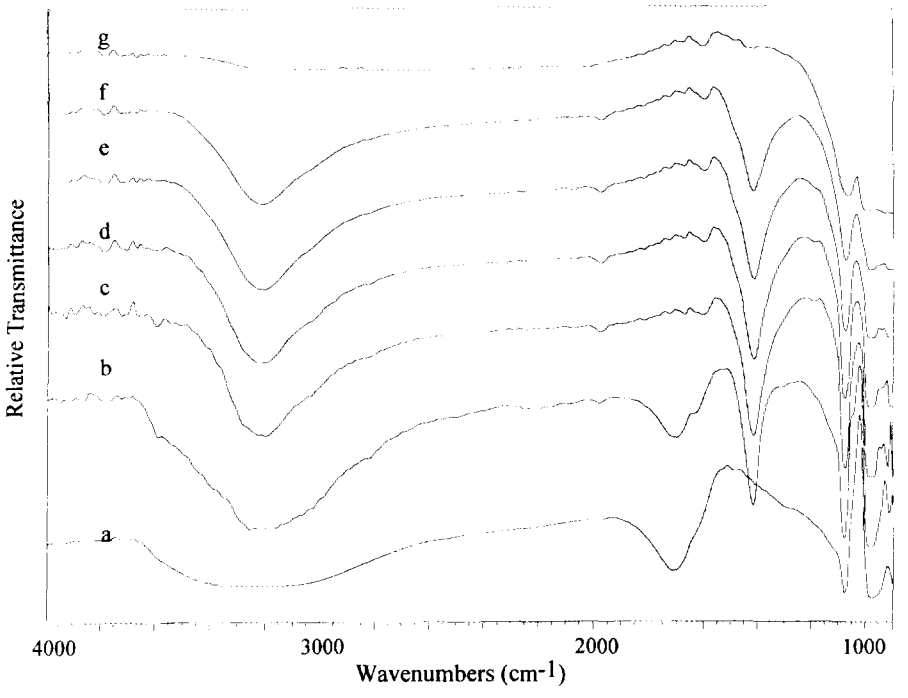

FIG. 5. IR spectra of $H_3PW_{12}O_{40} \cdot 6H_2O$ upon the following successive treatments: (a) $H_3PW_{12}O_{40} \cdot 6H_2O$ at 25°C; (b) after NH_3 saturation at 25°C (for 20 hr); (c) treated in N_2 at 150°C for 10 min; (d) treated in N_2 at 250°C for 10 min; (e) treated in N_2 at 350°C for 10 min; (f) treated in N_2 at 450°C for 10 min; and (g) treated in N_2 at 450°C for 5 hr.

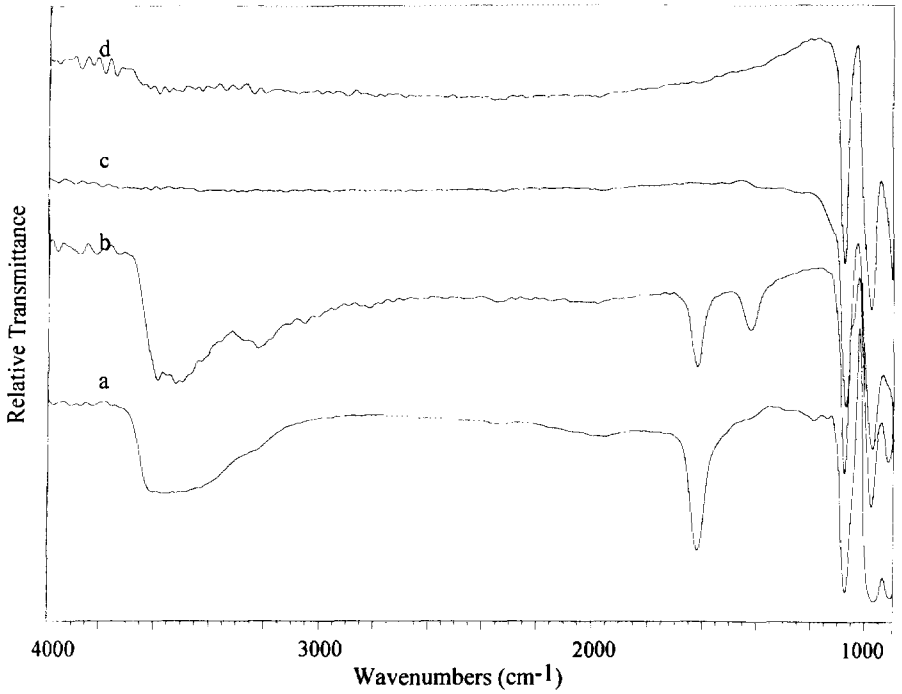

FIG. 6. IR spectra of $Na_3PW_{12}O_{40} \cdot xH_2O$ upon the following successive treatments: (a) sample at 25°C in N_2; (b) after treatment with NH_3 at 25°C for 30 min; (c) after desorption in N_2 at 200°C; and (d) after treatment with NH_3 at 25°C for 30 min.

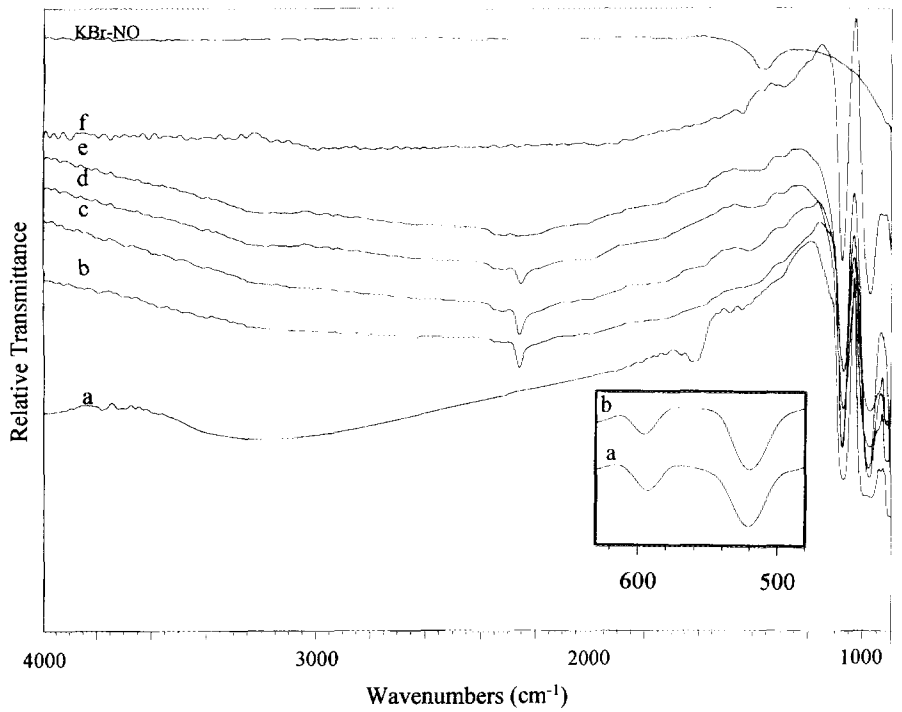

FIG. 7. IR spectra of $H_3PW_{12}O_{40} \cdot 6H_2O$ and its Na^+ salt upon the following successive treatments: (a) $H_3PW_{12}O_{40} \cdot 6H_2O$ in N_2 at 150°C for 2 hr; (b) upon NO treatment at 150°C for 10 min; (c) heated in N_2 at 250°C for 10 min; (d) heated in N_2 at 360°C for 10 min; (e) heated in N_2 at 410°C for 10 min; and (f) $Na_3PW_{12}O_{40} \cdot H_2O$ treated with NO at 150°C for 2 hr. Also included is the spectrum for a KBr pellet exposed to NO at 150°C.

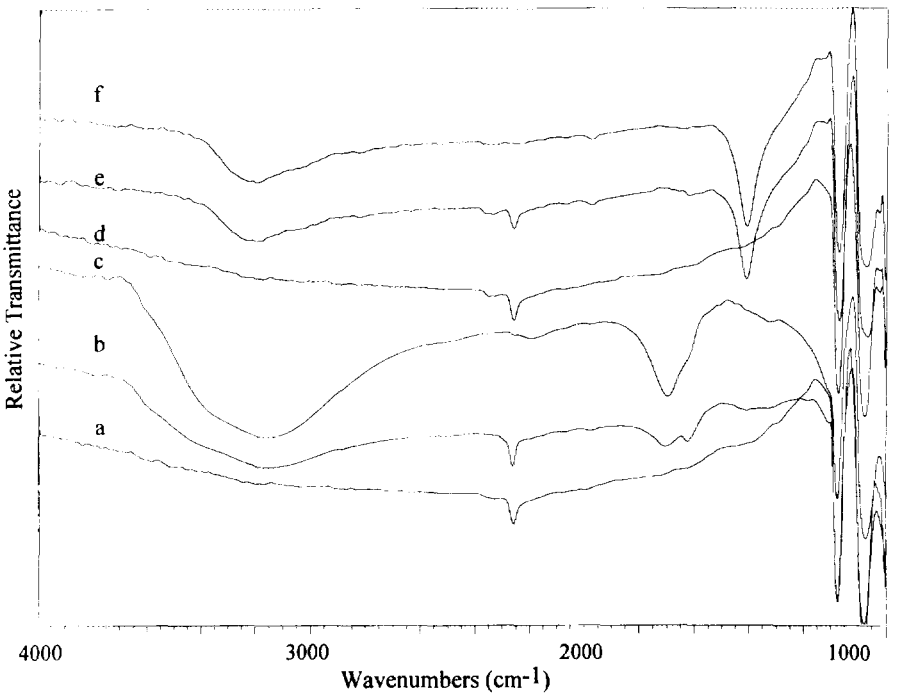

FIG. 8. IR spectra of $H_3PW_{12}O_{40} \cdot 6H_2O$ upon the following successive treatments: (a) saturated with NO at 150°C; (b) cooled to 50°C and treated with 0.02 atm H_2O for 15 min; (c) treated with 0.02 atm H_2O at 50°C for 1 hr; (d) heated to 150°C and saturated with NO; (e) treated with NH_3 at 150°C for 1 hr; and (f) treated with NH_3 at 150°C for 24 hr.

An experiment was also performed on NO absorption by $Na_3PW_{12}O_{40}$. The Na^+ salt was first heated to 150°C. As noted above, the weak residual Brønsted acidity in the Na^+ salt was essentially lost at 150°C. The heat-treated Na^+ salt was exposed to NO at 150°C. The resulting IR spectrum, also shown in Fig. 7, showed no absorption of NO by the salt. This result showed that the Brønsted acidity was needed for NO absorption in the heteropoly compound.

A number of competitive absorption experiments have been performed to determine conditions (i.e., temperature being the dominant condition) under which different molecules are favored for forming the linkages in the secondary structure of $H_3PW_{12}O_{40}$. Three linkage molecules were compared, H_2O, NH_3, and NO. At temperatures near and below 50°C, the following preference order was obtained: $NH_3 > H_2O > NO$. At near 150°C, the order was $NH_3 > NO > H_2O$, where NO became more preferred than H_2O. The results are summarized in Fig. 8. The results given in Fig. 8 only included pure gas results although the results using mixtures were the same. The concentrations were 3,000 ppm for NO, 3,000 ppm for NH_3, and 2% for H_2O.

DISCUSSION

Known Linkage Structures for Keggin Anions

The most extensively studied (and hence best known) linkage structures are the H_2O linkages in $H_3PW_{12}O_{40} \cdot 6H_2O$ and the Cs linkages in $Cs_3PW_{12}O_{40}$. The most common $H_3PW_{12}O_{40} \cdot 6H_2O$ compound (as used in this work) belongs to "type A" secondary structure (that is, the bcc structure) (25) containing the "α type" Keggin primary structure (33). As evidenced from the voluminous literature on reactions catalyzed by heteropoly compounds, the primary structure remains unchanged during reactions while the secondary structure may undergo dramatic changes. Therefore, understanding of the secondary structure is most important to the understanding of the reaction mechanism.

The secondary structure of $H_3PW_{12}O_{40} \cdot 6H_2O$ and the water linkages are shown in Fig. 9 (26). The structures with alcohol linkages are essentially the same as that of H_2O (5, 30). The structure with Cs linkages is of interest because of the following fundamental differences from the H_2O and alcohol linkages: Cs replaces the protons, it is ionic, and it is a large cation. The structure of $Cs_3PW_{12}O_{40}$ has been carefully determined (35). The structure is essentially the same as that of $H_3PW_{12}O_{40} \cdot 6H_2O$, with one Cs^+ (ionic radius = 1.67 Å) replacing each $H_5O_2^+$ linkage and hence a shorter bcc lattice constant of 11.83 Å.

Structure of the $(NOH)^+$ Linkages in $H_3PW_{12}O_{40} \cdot 3NO$

The stoichiometry of the NO-saturated heteropoly compound has been determined to be $H_3PW_{12}O_{40} \cdot 3NO$ ((1)

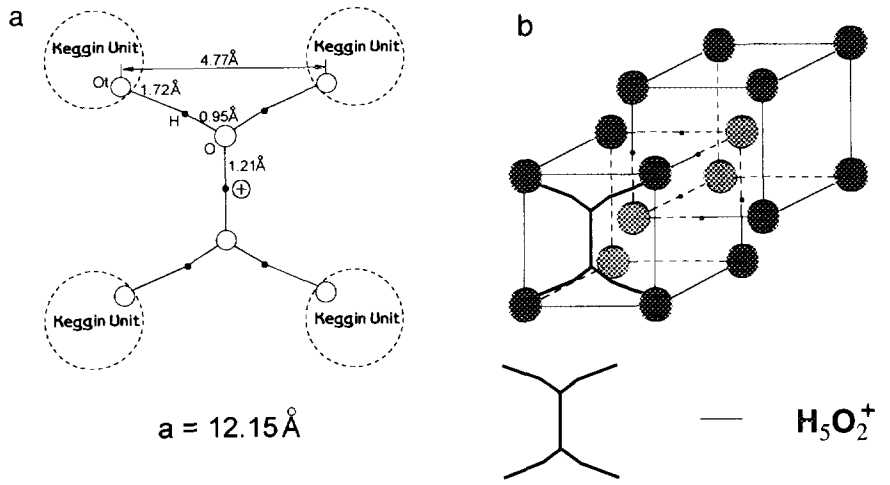

FIG. 9. (a) The $H_5O_2^+$ linkage joining four Keggin units in $H_3PW_{12}O_{40} \cdot 6H_2O$. The drawing is not to scale; the diameter of the Keggin unit is 10.43 Å. (b) The secondary structure is a bcc structure, where the dark spheres denote Keggin units and $H_5O_2^+$ is located on each face of the bcc.

and see above). From the NO desorption activation energy of 25.5 kcal/mol (determined from the TPD results), NO was clearly chemically bonded to the Keggin anions.

The IR spectrum of $H_3PW_{12}O_{40} \cdot 6H_2O$ showed the dominant band at 1710 cm^{-1} for the OH bending vibrations, which was attributed to $H_5O_2^+$. Upon substitution of H_2O by NO, the H_2O bands were replaced by a single band at 2270 cm^{-1}. Upon reversing the substitution, i.e., NO $\rightarrow$ H_2O, the IR spectra were also reproduced (Fig. 7). Also, upon substituting NO by NH_3, the 1450 cm^{-1} IR band (attributed to NH_4^+) replaced the 2270 cm^{-1} band (Fig. 8). All these results indicated that the protons remained in the structure and, more importantly, NO must have been bonded to the proton H^+. A further indication that NO was bonded to H^+ was seen in the treatment of the Na salt with NO (Fig. 9). When no residual H^+ remained in the Na salt, NO could no longer be bonded to the salt.

The nitrosonium ion (NO^+) was first observed by Angus *et al.* (35) in studying the Raman spectra of nitrosylsulfuric acid, where a fundamental frequency of 2330 cm^{-1} was attributed to NO^+. Since both the dipole moment and the polarizability of NO^+ change during vibration, the NO^+ vibration should be both Raman and IR active (36). A short time later, the IR absorption at 2300 cm^{-1} by NO^+ was found by Millen (37) in studying the ionization of dinitrogen tetroxide in nitric acid. Further studies (38) showed that the spectra were influenced by the environment of NO^+, e.g., 2300 cm^{-1} for NO^+ in solid nitrosonium hydrogen sulfate and 2313 cm^{-1} in aqueous sulfate solution. Also, a protonated form, $NH_2O_4^+$, yielded substantially lower IR frequencies (39).

Based on the TGA and, more importantly, the nitrogen mass balance results, the linkages were NO rather than NO_2, as discussed above. It is also important to determine whether NO^+ or NO_2^+ (23) was bonded to $H_3PW_{12}O_{40}$. The NO_2^+ ion would yield an IR band at 570 cm^{-1} for O—N—O bending and a band at 2350 cm^{-1} for N—O asymmetric stretching (40). The NO_2^+ stretching frequency is close to that for NO^+. As mentioned, CaF_2 windows and a CaF_2 sample holder were used for the IR study. In order to observe the region for the NO_2^+ bending frequency, a separate *in situ* IR experiment was conducted employing Si windows and a Si sample holder, which extended the IR spectra to 400 cm^{-1}. The results were added to Fig. 7 as an inset. It is clear that no band appeared at near 570 cm^{-1}.

Based on all the IR results in our study and from the literature and the TPD data, it is only reasonable to assign the 2270 cm^{-1} band to a protonated nitrosonium ion, $(NOH)^+$. Moreover, since the 980 cm^{-1} IR band did not undergo splitting, the $(NOH)^+$ should be connected to the terminal oxygen (O_t) on the Keggin anion, so the W = O_t vibration was not influenced.

As discussed above, the linkage structure of H_2O and Cs^+ linkages are well understood. Figure 9a shows the water linkages and the lengths of the covalent bonds involved in the linkage (26). The resulting bcc lattice constant of 12.15 Å was in agreement with the XRD data. For the NOH linkages, there were three possible linkage structures, shown in Figs. 10a–10c. Standard and appropriate covalent bond lengths were used in the calculations shown in Figs. 10a–10c. The calculation for the ionic $(NOH)^+$ linkage needs an explanation. The covalent bond lengths of 1.20 Å for the N—O bond and 1.73 Å for the O—H bond were used within the linkage. At the two ends, the sizes of the two end atoms should be included for calculating the minimum diameter of the ionic linkage. Thus the standard atomic radii of 0.31 Å for H and 0.74 Å for N were used in the calculation, resulting in 11.74 Å for the

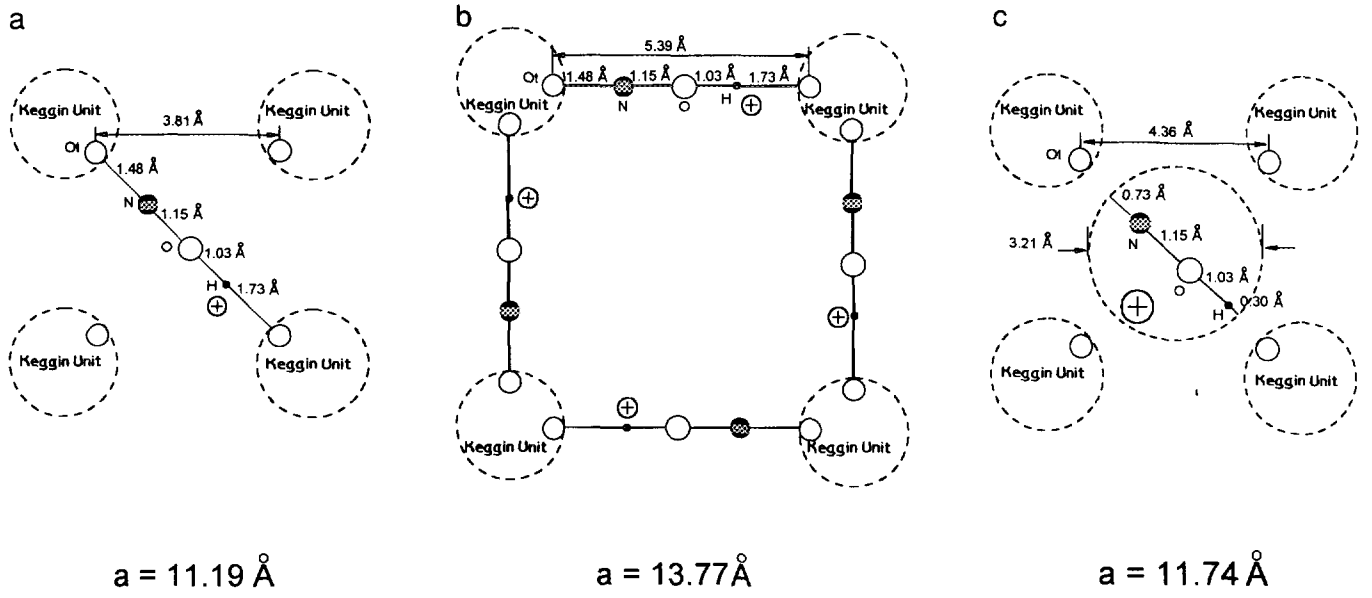

FIG. 10. Three possible linkage structures for $H_3PW_{12}O_{40} \cdot 3NO$. The drawings are not to scale; the diameter of the Keggin unit is 10.43 Å. (a) With diagonal NOH linkage covalently bonded to terminal oxygen of Keggin units. (b) NOH covalently bonded to each side. (c) The $(NOH)^+$ ion bonded to 4 Keggin units, resembling that in the Cs^+ salt. Structure (c) is the correct one based on XRD data as discussed in text.

diameter of the $(NOH)^-$ ion linkage. Based on the bond lengths, it is clear that the ionic $(NOH)^+$ linkage yielded the closest value for the bcc lattice constant of 11.74 Å, compared to that of the XRD data, 11.68 Å. Moreover, for the two NOH covalently bonded linkages (a and b), it would be expected to see IR frequencies of O—N = O bonds, which were typically near 1400 cm^{-1}. The total absence of IR bands in this region further indicated that the ionic linkage (Fig. 10c) was the correct structure.

Figure 11 shows the three-dimensional secondary structure of the $H_3PW_{12}O_{40} \cdot 3NO$ with the ionic NOH linkages. This structure closely resembles that of the Cs salt, $Cs_3PW_{12}O_{40}$. Two sets of interpenetrating cubic structures form the bcc structue that is shown by XRD.

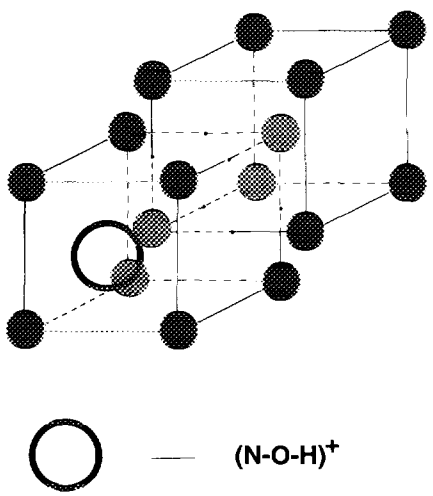

FIG. 11. The bcc (with respect to Keggin units) secondary structure of $H_3PW_{12}O_{40} \cdot 3NO$. The $(NOH)^+$ is located on each face of the bcc.

Two points are worth noting. Based on the linkage molecules for the heteropoly compounds reported in the literature, such as H_2O (26), alcohols (30), $(C_2H_5)_2O$ (30), NH_3 (31), amines (29), pyridine (19), and the NO linkage studied in this work, and the fact that salts cannot form linkages with these molecules, it seems that the ability to be protonated is a prerequisite for the molecule to form linkages. The second point is concerned with the activation of the NO molecule, and hence is of catalytic importance. The IR vibration frequency of the NO linkages is at 2270 cm^{-1}, which represents a considerable decrease from the frequency of a nitrosonium NO^+ ion, 2330 cm^{-1}. This decrease reflects a weakening of the N—O bond due to protonation and may serve as a clue for the mechanism of decomposition into N_2 that we observed earlier (1).

ACKNOWLEDGMENT

This work was supported by the New York State Energy Research and Development Authority, Project 4054-ERTER-ER-95.

REFERENCES

1. Yang, R. T., and Chen, N., *Ind. Eng. Chem. Res.* **33**, 825 1994).
2. Pope, M. T., "Heteropoly and Isopoly Oxometalates." Springer-Verlag, New York, 1983.
3. Keggin, J. F., *Proc. R. Soc. A* **144**, 75 (1935).

4. Misono, M., *Catal. Rev. Sci. Eng.* **29,** 269 (1987).
5. Ono, Y., *in* "Perspectives in Catalysis" (J. M. Thomas and K. I. Zamaraev, Eds.). Blackwell, London, 1992.
6. Sorensen, C. M., and Weber, R. S., *J. Catal.* **142,** 1 (1993).
7. Vaughan, J. S., O'Connor, C. T., and Fletcher, J. C. Q., *J. Catal.* **147,** 441 (1994).
8. Ohtsuka, R., and Kobayashi, J., *Bull. Chem. Soc. Jpn.* **63,** 2076 (1990).
9. Albonetti, S., Cavani, F., Trifiro, F., Gazzano, M., Koutyrev, M., Aissi, F. C., and Abonkais, A., *J. Catal.* **146,** 491 (1994).
10. Tsigdinos, G. A., *Top. Curr. Chem.* **76,** 1 (1978).
11. Baba, T., Ono, Y., Ishimoto, T., Moritaka, S., and Tanooka, S., *Bull. Chem. Soc. Jpn.* **58,** 2155 (1985).
12. Dun, J. W., Gulari, E., and Streusand, B., *Appl. Catal.* **21,** 61 (1986).
13. Kohevnikov, I. V., and Matveev, K. I., *Appl. Catal.* **5,** 135 (1983).
14. Soria, J., Conesa, J. C., Lopez Granados, M., Mariscal, R., Fierro, J. L. G., Garcia de la Banda, J. F., and Heinemann, H., *J. Catal.* **120,** 457 (1989).
15. Mohana Rao, K., Gobetto, R., Iannibello, A., and Zecchina, A., *J. Catal.* **119,** 512 (1989).
16. Konishi, Y., Sakata, K., Misono, M., and Yoneda, Y., *J. Catal.* **77,** 169 (1982).
17. Himeno, S., Osakai, T., and Saito, A., *Bull. Chem. Soc. Jpn.* **64,** 21 (1991).
18. Casavini, D., Centi, G., Jiru, P., Lena, V., and Tvaruzkova, Z., *J. Catal.* **143,** 325 (1993).
19. Misono, M., Mizuno, N., Katamura, K., Kasai, A., and Konishi, Y., *Bull. Chem. Soc. Jpn.* **55,** 400 (1982).
20. Misono, M., Sakata, K., Yoneda, Y., and Lee, Y. W., "Proceedings 7th International Congress on Catalysis, Tokyo, 1980" (T. Seiyama and K. Tanabe, Eds.), p. 1047. Elsevier, Amsterdam, 1981.
21. Saito, Y., and Niiyama, H., *J. Catal.* **106,** 329 (1987).
22. Hibi, T., Takahashi, K., Okuhara, T., Misono, M., and Yoneda, Y., *Appl. Catal.* **24,** 69 (1986).
23. Bélanger, R., and Moffat, J. B., *J. Catal.* **152,** 179 (1995).
24. Hayashi, H., and Moffat, J. B., *J. Catal.* **81,** 61 (1983).
25. Cvetanovic, R. J., and Amenomiya, Y., *Catal. Rev. Sci. Eng.* **6,** 21 (1972).
26. Brown, G. B., Noe-Spirlet, M. R., Busing, W. R., and Levy, H. A., *Acta. Crystallogr., Sect. B* **33,** 1038 (1977).
27. Rocchiccioli-Deltcheff, C., Fournier, M., Frank, R., and Thouvenot, R., *Inorg. Chem.* **22,** 207 (1983).
28. Okuhara, T., Kasai, A., Hayakawa, N., Yoneda, Y., and Misono, M., *J. Catal.* **83,** 121 (1983).
29. Furuta, M., Sakata, K., Misono, M., and Yoneda, Y., *Chem. Lett. (Jpn)* **31** (1979).
30. Lee, K. Y., Mizuno, N., Okuhara, T., and Misono, M., *Bull. Chem. Soc. Jpn.* **62,** 1731 (1989).
31. Seo, G., Lim, J. W., and Kim, J. T., *J. Catal.* **114,** 469 (1988).
32. Kung, M. C., and Kung, H. H., *Catal. Rev. Sci. Eng.* **27,** 425 (1985).
33. Evans, H. T., Jr., *Perspect. Struct. Chem.* **4,** 1 (1971).
34. Santos, J. A., *Proc. R. Soc. A* **150,** 309 (1935).
35. Angus, W. R., Leckie, A. H., and Ramsay, W., *Proc. R. Soc. A* **149,** 327 (1935).
36. Nakamoto, K., "Infrared and Raman Spectra of Inorganic and Coordination Compounds," p. 22. Wiley, New York, 1986.
37. Millen, D. J., *J. Chem. Soc.,* 2600 (1950).
38. Goulden, J. D. S., and Millen, D. J., *J. Chem. Soc.,* 2620 (1950).
39. Millen, D. J., and Watson, D., *J. Chem. Soc.,* 259 (1957).
40. Laane, J., and Ohlsen, J. R., *Prog. Inorg. Chem.* **27,** 465 (1980).